First principles study of the magnetic properties of LaOMnAs

Shuai Dong,[1,2,3,a)] Wei Li,[4,5] Xin Huang,[1] and Elbio Dagotto[2,3]
[1]*Department of Physics, Southeast University, Nanjing 211189, China*
[2]*Department of Physics and Astronomy, University of Tennessee, Knoxville, Tennessee 37996, USA*
[3]*Materials Science and Technology Division, Oak Ridge National Laboratory, Oak Ridge, Tennessee 37831, USA*
[4]*Shanghai Center for Superconductivity and State Key Laboratory of Functional Materials for Informatics, Institute of Microsystem and Information Technology, Chinese Academy of Sciences, Shanghai 200050, China*
[5]*Department of Physics, Fudan University, Shanghai 200433, China*

(Presented 6 November 2013; received 19 September 2013; accepted 5 December 2013; published online 7 March 2014)

Recent experiments reported giant magnetoresistance at room temperature in LaOMnAs. Here, a density functional theory calculation is performed to investigate magnetic properties of LaOMnAs. The ground state is found to be the G-type antiferromagnetic order within the *ab* plane but coupled ferromagnetically between planes, in agreement with recent neutron investigations. The electronic band structures suggest an insulating state which is driven by the particular G-type magnetic order, while a metallic state accompanies the ferromagnetic order. This relation between magnetism and conductance may be helpful to qualitatively understand the giant magnetoresistance effects. © *2014 AIP Publishing LLC*. [http://dx.doi.org/10.1063/1.4867757]

Since the discovery of high-temperature superconductivity in fluorine-doped LaOFeAs,[1] several Fe-based pnictide and chalcogenide compounds have been systematically studied.[2–5] Recently, the Mn-based oxypnictides *R*OMnAs (*R* is a rare earth, e.g., La, Nd, Sm) that present a similar crystal structure as the materials mentioned above have also been synthesized and studied experimentally.[6–13] In contrast to their Fe-based cousins, at least, until now, these Mn-based oxypnictides have not shown any evidence of superconductivity even in doped cases. Instead, giant or even colossal magnetoresistance effects at room temperature have been observed in these compounds,[10–13] which reminds us of the well-known phenomenology of the colossal magnetoresistive manganites (Mn-based oxides) with the perovskite structures.[14]

Neutron studies have revealed that the magnetic ground state of *R*OMnAs is different from the isostructural *R*OFeAs.[8,13] Different from the isostructural LaOFeAs which owns a stripe-like antiferromagnetic (AFM) state (as in the CA one shown in Fig. 1), *R*OMnAs shows a conventional in-plane G-type AFM order where all NN spins are antiparallel in-plane.[13] This magnetic order is also different from magnetic orders in other Fe-based pnictides and chalcogenides, e.g., the bi-stripe AFM order found in FeTe[15] and the block-AFM order predicted in KFe_2Se_2.[16]

To understand the basic physical properties of *R*OMnAs, here we perform a density functional theory (DFT) calculation to investigate the electronic structures of LaOMnAs, especially its magnetic properties. Theoretically, LaOMnAs is simpler than NdOMnAs and SmOMnAs within the DFT framework since La^{3+} is non-magnetic (NM). Fortunately, the most attractive properties of *R*OMnAs, e.g., its magnetoresistive, does not rely on the magnetism of the rare-earth component. Thus, the undoped LaOMnAs provides a good starting point to study the exotic giant (or colossal) magnetoresistance of *R*OMnAs. Although Xu *et al.* have already conducted a pioneering DFT calculation on LaO *M*As (*M* = V-Cu),[17] the real LaOMnAs compound was experimentally studied in detail two years later.[11] Thus, there are some non-negligible differences between the early DFT predictions and the experimentally

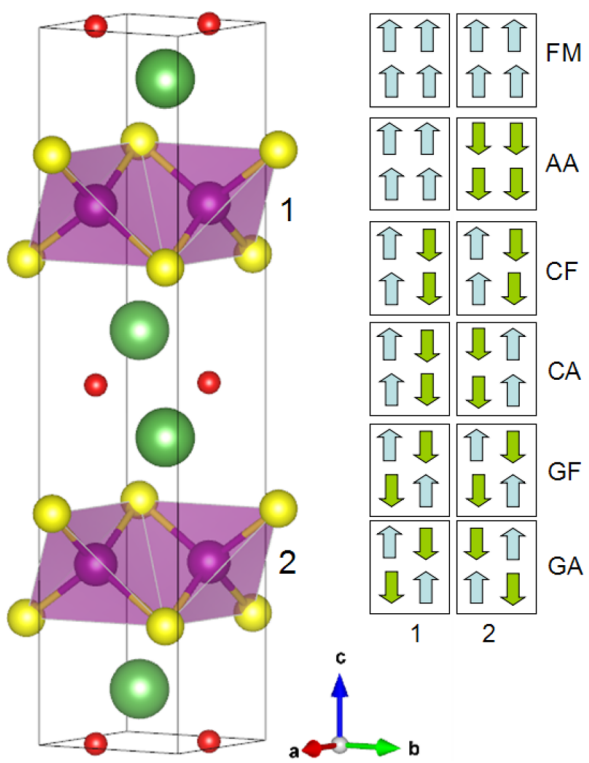

FIG. 1. *Left*: Crystal structure of a unit cell of LaOMnAs, which contains four chemical units. Elements: La (green); O (red); Mn (purple); As (yellow). *Right*: Sketches of magnetic orders of Mn. The NN layer indexes are denoted as 1 and 2. The magnetic ground state of *R*OFeAs is CA, while it is GA or GF for *R*OMnAs.

[a)]Author to whom correspondence should be addressed. Electronic mail: sdong@seu.edu.cn.

unveiled facts, such as the lattice constants. Later, a DFT calculation by Kayanuma *et al.* emphasized the band gap of LaOMn X (X = P, As, and Sb) but did not focus on the magnetism. Thus, it is necessary to perform a careful DFT calculation on LaOMnAs with the help of current experimental information and compare the new results against those previous pioneering theoretical works.

The crystal structure of LaOMnAs is tetragonal ZrCuSiAs-type, with the space group $P4/nmm$,[13] as shown in Fig. 1. Each Mn cation is caged by an As tetrahedron. Also each Mn-As layer contains a square Mn lattice which is effectively isolated from the La-O layer, defining a two-dimensional (2D) network of Mn cations.

The DFT calculation reported here was performed based on the projected augmented wave pseudopotentials using the Vienna *ab initio* simulation package (VASP).[18–20] The electron-electron interaction is described using the generalized gradient approximation (GGA) method. The energy cutoff is 500 eV. The experimental crystal structure (lattice constants *a*-*b*-*c* and atomic positions) at 5 K is adopted.[13] The Γ-center *k*-mesh is $9 \times 9 \times 2$ for one unit cell or $6 \times 6 \times 2$ for two unit cells (only for the CA and CF cases as shown in Fig. 1).

To determine the ground state, several possible magnetic orders have been tested, as noted in Fig. 1. The DFT results are summarized in Table I. The G-type AFM state has the lowest energy. Here, both GA and GF are in-plane G-type AFM for each layer, but coupled antiferromagnetically and ferromagnetically between NN layers, respectively. The energy difference between GA and GF is of the order of 0.1 meV, which is beyond the precision of current DFT calculations. Thus, those states are considered to be degenerate within our calculation. Similar degenerate characteristics also exist between the CF and CA cases. Also, a tiny difference occurs between the FM and AA cases. Thus, from these energy differences, it is safe to conclude that the exchange coupling between NN layers are very weak ($|J_c| \leqslant 1.75$ meV with normalized spins $|S| = 1$). To further confirm this point, all atomic positions were relaxed for the GF and GA cases: In this case, the energy difference remained of the order of 0.1 meV. Our results agree with the neutron data with regards to the in-plane G-type antiferromagnetism.[13] The experiments found that LaOMnAs is GF while NdOMnAs is GA possibly due to the influence of the Nd moments, which also suggested the proximity in energy between those two states.

TABLE I. DFT results. Here, the FM state is the reference state for the energy. The energy per Mn is in units of meV. The magnetic moments are in units of μ_B/Mn calculated using Wigner–Seitz spheres as specified by VASP (not very accurate). The values in brackets for the FM case have been calculated from the total magnetization. The band gaps are in units of eV.

Magnetic order	Energy	Moment	Band gap
NM	546.5	0	-
FM	0	3.390 (3.559)	-
AA	3.5	3.338	-
CF	−313.5	3.615	0.429
CA	−313.9	3.614	0.428
GF	−452.7	3.596	0.524
GA	−452.6	3.595	0.524

All calculated magnetic states present strong local moments: About $3.3 - 3.6\,\mu_B$ per Mn, which is quite close to (only a little higher than) the experimental values ($\sim 3.34\,\mu_B$ per Mn at 2 K).[13] When the Hubbard U is considered using the GGA + U method, the local moment can further increase to more than $4\,\mu_B$ per Mn (Fig. 2(c)) due to the enhanced localization of 3*d* electrons. According to these results, it seems that the GGA method may be even better than the GGA + U one for the LaOMnAs. And these results suggest a high-spin state for Mn due to the strong Hund exchange although the moments are not ideally large ($5\,\mu_B$ per Mn).

The band structure of the GA state (i.e., the experimentally observed state) is shown in Fig. 2(a). Here, the atomic positions have been relaxed in the calculation. The top of the valence bands is located at the Γ point, while the bottom of the conducting bands is at the M point. Therefore, LaOMnAs is an indirect semiconductor, in agreement with experiments.[9] Also, in experiments, the electronic doping, e.g., F doping at the oxygen site, will create Fermi surface pockets around the M point first, while hole doping (e.g., Ca doping at the La site) will create Fermi surface pockets around the Γ point. This is different from the case of LaOFeAs, which is a bad metal displaying both electron and hole pockets at the Fermi surface in the undoped case.

The element-resolved DOS further confirms that the bands near the Fermi level are mostly from the Mn's 3*d* orbitals, which hybridize with the As's 4*p* orbitals, as shown in Fig. 2(b). By contrast, La and O do not contribute significantly to these bands. Then, in future studies, tight-binding models based on multi-3*d*-orbitals as widely used for Fe-based superconductors can also be used for *R*OMnAs, with only appropriate modifications in the specific values of the model parameters (such as the crystal-field splitting, hopping amplitudes, electron filling, Hubbard U, and Hund coupling).[4]

In the present study, the calculated band gap (0.524 eV) is lower than the experimental gap measured using optical

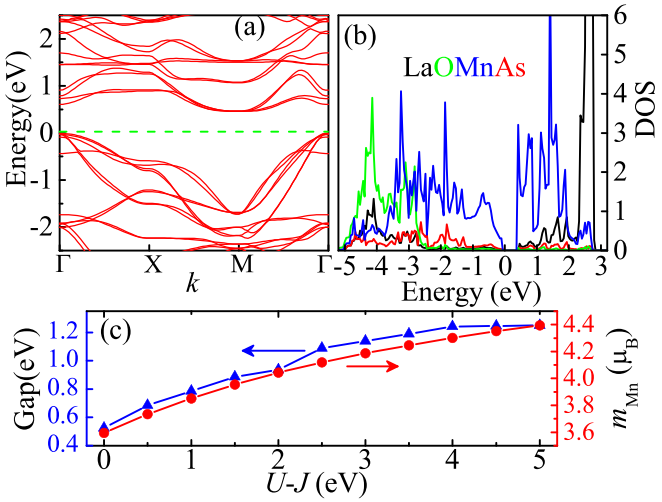

FIG. 2. (a) Band structure near the Fermi level for the experimentally observed GF state. (b) The element-resolved DOS. According to (a) and (b), the bands near the Fermi level originate mainly from the manganese 3*d* orbitals, which hybridize with the arsenic 4*p* orbitals. (c) The band gap (left axis) and local moment of each Mn (right axis) as a function of the Hubbard coupling strength acting on the Mn 3*d* electrons. Here *U*–*J* is fixed as 8 eV for the La 4*f* electrons except for the non-correlated ($U - J = 0$) limit.

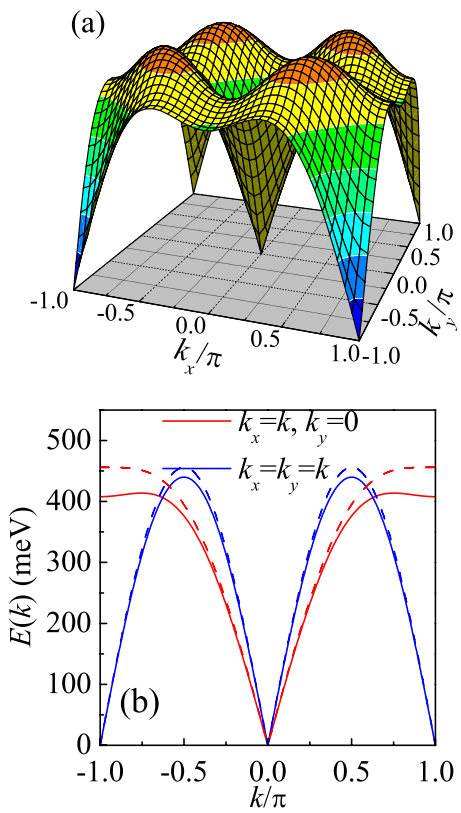

FIG. 3. Spin wave dispersions. (a) In the whole 2D first Brillouin zone. (b) Along two special lines: (1) $k_y = 0$; (2) $k_x = k_y$. Here the x–y frame is based on the square Mn lattice (the links between NN Mn's). The broken curves are dispersions without J_2 for comparison.

absorption (namely ~1.4 eV, but this value may be not very accurate due to a strong absorption tail) for LaOMnAs thin films.[9] In fact, the earliest DFT calculation gave an even smaller gap value (0.2 eV),[17] The GGA+ U method, incorporating the effective Hubbard parameter $U - J = 1.5$ eV for the Mn 3d and 8 eV for the La 4f electrons, gave a larger gap (0.878 eV), but it was still smaller than the experimental one.[9] Here, the GGA+ U method is also tested by tuning the values of U–J to analyze the effect of the Hubbard-type correlation. As shown in Fig. 2(c), the band gap increases with the effective Hubbard parameter U–J for Mn, as expected. For example, the gap is about 1.24 eV when $U - J = 4$ eV, which is already large enough for Mn. In spite of this improvement, the gap width tends to saturation with further increasing U–J, and it is still below the experimental value. Further increase of U–J for the La 4f electrons up to 11 eV does not alter this result (not shown here). This underestimate of the band gap may be due to the well-known deficiencies of DFT that tend to favor metallic tendencies, or the inaccuracy of the experimental measurements, or the difference between thin films and bulk properties.

From the energy difference between the various magnetic states, it is straightforward to extract the superexchange coefficients by mapping the system to a classical 2D Heisenberg model with the nearest-neighbor exchange J_1 and next-nearest-neighbor exchange J_2: From Table I and using normalized spins, it is known that $J_1 = 113.2 - 114$ meV and $J_2 = 21.8 - 22.3$ meV, both of which are AFM and much stronger than the aforementioned inter-layer coupling. The NN exchange is the dominant one while the NNN exchange is only about 1/5 of the NN one, which is different from the case of LaOFeAs where J_2/J_1 was larger. The physical mechanism of such strong AFM couplings can be understood by the semi-empirical Goodenough–Kanamori rule considering the half-filled 3d level of the high-spin Mn^{2+} ion.[21,22] This strong J_1 is responsible for the high Néel temperature 317 K as well.[11,13]

By using these exchanges, the spin-wave dispersions can be calculated analytically. As shown in Fig. 3, the spin wave dispersions are typical 2D G-type AFM ones. Due to the NNN exchange J_2, the dispersions become a little softer near the Brillouin boundary when $k_x = 0$ or $k_y = 0$.

In summary, the oxypnictide LaOMnAs is studied using the first principles calculation. The in-plane magnetic ground state is confirmed to be the conventional G-type antiferromagnetism, while the coupling between layers is very weak. The dominant exchange coupling is the nearest-neighbor one while the next-nearest neighbor coupling is relatively weak. The conductance of LaOMnAs depends on the magnetic order, which may be helpful to understand the giant magnetoresistance effects observed in these materials.

Work was supported by the 973 Projects of China (No. 2011CB922101) and NSFC (Nos. 11274060 and 51322206). E.D. was supported by the National Science Foundation Grant No. DMR-1104386.

[1]Y. Kamihara, T. Watanabe, M. Hirano, and H. Hosono, J. Am. Chem. Soc. **130**, 3296 (2008).
[2]D. C. Johnston, Adv. Phys. **59**, 803 (2010).
[3]G. R. Stewart, Rev. Mod. Phys. **83**, 1589 (2011).
[4]E. Dagotto, Rev. Mod. Phys. **85**, 849 (2013).
[5]P. C. Dai, J. P. Hu, and E. Dagotto, Nat. Phys. **8**, 709 (2012).
[6]Y. Shiomi, S. Ishiwata, Y. Taguchi, and Y. Tokura, Phys. Rev. B **84**, 054519 (2011).
[7]J. W. Simonson, K. Post, C. Marques, G. Smith, O. Khatib, D. N. Basov, and M. C. Aronson, Phys. Rev. B **84**, 165129 (2011).
[8]A. Marcinkova, T. C. Hansen, C. Curfs, S. Margadonna, and J. W. G. Bos, Phys. Rev. B **82**, 174438 (2010).
[9]K. Kayanuma, H. Hiramatsu, T. Kamiya, M. Hirano, and H. Hosono, J. Appl. Phys. **105**, 073903 (2009).
[10]E. J. Wildman, J. M. S. Skakle, N. Emery, and A. C. Mclaughlin, J. Am. Chem. Soc. **134**, 8766 (2012).
[11]N. Emery, E. J. Wildman, J. M. S. Skakle, G. Giriat, R. I. Smith, and A. C. Mclaughlin, Chem. Commun. **46**, 6777 (2010).
[12]Y.-L. Sun, J.-K. Bao, Y.-K. Luo, C.-M. Feng, Z.-A. Xu, and G.-H. Cao, EPL **98**, 17009 (2012).
[13]N. Emery, E. J. Wildman, J. M. S. Skakle, A. C. Mclaughlin, R. I. Smith, and A. N. Fitch, Phys. Rev. B **83**, 144429 (2011).
[14]E. Dagotto, T. Hotta, and A. Moreo, Phys. Rep. **344**, 1 (2001).
[15]S. Li, C. de la Cruz, Q. Huang, Y. Chen, J. W. Lynn, J. Hu, Y.-L. Huang, F.-C. Hsu, K.-W. Yeh, M.-K. Wu, and P. Dai, Phys. Rev. B **79**, 054503 (2009).
[16]W. Li, S. Dong, C. Fang, and J. P. Hu, Phys. Rev. B **85**, 100407 (2012).
[17]G. Xu, W. Ming, Y. Yao, X. Dai, S.-C. Zhang, and Z. Fang, EPL **82**, 67002 (2008).
[18]P. E. Blöchl, O. Jepsen, and O. K. Andersen, Phys. Rev. B **49**, 16223 (1994).
[19]G. Kresse and J. Hafner, Phys. Rev. B **47**, 558 (1993).
[20]G. Kresse and J. Furthmüller, Phys. Rev. B **54**, 11169 (1996).
[21]J. B. Goodenough, J. Phys. Chem. Solids **6**, 287 (1958).
[22]J. Kanamori, J. Phys. Chem. Solids **10**, 87 (1959).